

# Development of a High Accuracy Pointing System for Maneuvering Platforms

Joseph M. Strus, *SRI International*  
Michael Kirkpatrick, *SRI International*  
James W. Sinko, *SRI International*

## BIOGRAPHY

Joseph M. Strus is a Systems Analyst at SRI International where he has worked on precision navigation applications since 2001. His interests are GPS, GPS/INS and estimation theory. Previously, he was a GPS Systems Engineer with the Government Systems Division of Rockwell Collins. Dr. Strus received his B.S. and Ph.D. (Mathematics) from the University of Illinois at Urbana-Champaign and holds several GPS related patents.

Michael Kirkpatrick is currently a Senior Research Engineer at SRI International, where he has been involved in hardware and software systems design and development since 1985.

James W. Sinko is a Principal Engineer at SRI International. He received his B.S. (Engineering Science) and M.S.E.E. from Stanford University, and his Ph.D. (EE) from the University of Rochester. Dr. Sinko has been with SRI since 1967, working with radar and aircraft systems. For the last 13 years, he has been working with precision GPS for military and civil applications.

## ABSTRACT

This paper describes the general design and testing of attitude systems for moving vehicles capable of  $0.1^\circ$  3-D pointing accuracy, small external form factor, roll-on capability and reasonable cost. Applications include simulation and training systems, antenna pointing and airborne radar. The systems combine tactical grade inertial measurement units (IMU) with GPS. In particular, the Honeywell HG1900 MEMS inertial unit will be discussed and compared with a Litton LN-200. The paper will discuss the filter modifications used to incorporate the Honeywell IMU, an assessment of the error characteristics of the Honeywell MEMS IMU and the overall performance achieved versus the above requirements.

Two different truth systems for verifying the accuracy of the system were used. For ground tests, the GPS/INS systems were mounted on a 4.6 meter boom on a minivan. The boom was designed and engineered to precise tolerances in a machine shop. The boom has carefully mounted L1/L2 GPS antennas on each end. The resulting GPS attitude system has an estimated accuracy of  $0.06^\circ$  in azimuth, and  $0.15^\circ$  in pitch. The boom also has a telescopic rifle scope so that distant landmarks can be sighted with an estimated accuracy of  $0.015^\circ$ .

With proper maneuvers, we have observed the LN-200 based system to provide accuracies of  $0.06^\circ$  in azimuth and  $0.03^\circ$  in pitch. When the system was stationary the azimuth accuracy deteriorated at a rate of about  $0.5^\circ$  per hour. The HG1900 based unit attained the same level of accuracy, but had a stationary drift rate of approximately  $2^\circ$  per hour.

## INTRODUCTION

SRI International (SRI) has recently considered requirements for pointing systems for a variety of maneuvering platforms. These platforms include airborne systems (UAVs, aircraft), surface based vehicles (tanks, HUMVEES) and marine vessels. The goal was to obtain  $0.1^\circ$  pointing accuracy. Several design options were considered. A stand-alone navigation grade IMU was considered too expensive and heavy but is clearly advantageous in that it is more immune to GPS outages. A magnetic compass based solution was considered too problematic due to calibration and accuracy issues. After other design trades were considered, the path forward was limited to tactical grade inertial measurement units combined with GPS. Several different tactical grade IMUs were then considered for integration into a flexible software package previously developed at SRI for position and attitude tracking of large parachute pallet loads.

A secondary goal was to establish a truth system to verify pointing accuracy of the developed system. The goals of the truth system were for approximately  $0.06^\circ$  for kinematic applications and  $0.02^\circ$  for static applications. Moreover, it was desired that all biases between the units under test and the truth system would be less than  $0.01^\circ$ . Providing truth at this level of accuracy presents difficulties, however. Optical systems can easily attain this level of accuracy for static tests. For dynamic tests a high speed camera system with excellent timing coupled with accurate GPS positions and a view of distant landmarks could be used, but processing would be laborious. This approach was not pursued. A GPS attitude system works well, but attaining the necessary accuracy requires a long baseline. As will be described below, a synergistic effect between the IMU/GPS systems and the GPS attitude system led to a better than expected performance for the GPS attitude system under dynamic conditions.

Several ground based tests were done with two separate GPS/IMU units mounted on a boom on a minivan. In one test, the units were configured identically and the second unit was used as an additional statistical data point. In other tests, the units were configured differently and direct comparisons were then made.

The first part of this paper presents the component analysis and differences for the Honeywell MEMS versus the LN-200. Then the design and architecture for the system and the associated GPS/INS navigation processing software are considered. Next we discuss implementation

differences for the various components. After that the truth systems developed at SRI will be considered. Finally, we discuss the tests performed, truth data analysis methodology and results.

## IMU UNITS EVALUATED

The IMUs evaluated were the Northrop Grumman LN-200 and the Honeywell HG-1900. The LN-200 uses three fiber optic gyros. The particular model of the LN-200 is referred to as A=2. This corresponds to approximately a mid-range LN-200. The Honeywell HG1900 incorporates MEMS gyros and as such has relatively lower power consumption.

Table 1 shows relevant gyro parameters for the two IMUs used. Terminology for each unit is verbatim from the manufacturer's literature [Litton, 2000; Honeywell, 2004].

The evaluation methodology was to establish a gyro simulation with a consistent power spectral density and Allan variance with each unit under test; to do this, multiple long runs of greater than 24 hours were made. These runs were used to perform the Allan variance analysis. Short term runs of less than an hour were used to establish the turn-on bias. The accelerometer component of the analysis is left out as most interesting at this point are the gyros. Moreover, the accelerometer performance of the units is not remarkably different.

**Table 1:** Relevant Manufacturer's Specifications

LN-200 311875-240207		HG-1900 BA99	
Gyro bias stability, $^\circ/\text{hr}$ , $1 \sigma$ (100 sec correlation time)	0.65	Bias in-run stability, $^\circ/\text{hr}$ , $1 \sigma$	10
Random walk, $^\circ/\sqrt{\text{hr}}$	0.15	Angular random walk, $^\circ/\sqrt{\text{hr}}$	0.125
Scale factor accuracy, PPM, $1 \sigma$	100	Scale factor linearity, PPM, $1 \sigma$ (input $> 11.11^\circ/\text{sec}$ )	450
Drift (bias), $^\circ/\text{hr}$ , $1 \sigma$	3.0	Bias repeatability, $^\circ/\text{hr}$ , $1 \sigma$	30

## ANALYSIS DESCRIPTION

The units were set up to run stationary at a more or less constant temperature. The temperature control system in use can be assumed to keep the room temperature within 5° F. The units were set to run over several days. In general, no attempt was made to estimate the absolute bias. As a result, the units were oriented pointing more or less north.

Both units output data at nominally 100 Hz. Test software was loaded into the units which summed raw  $\Delta v$  and  $\Delta \theta$  data over one hundred samples and output the result.

The principal method to measure gyro stability used here will be the Allan variance. The Allan variance has previously been used to study gyro stability in several applications [Hou, 2004]. The Allan variance is defined in IEEE [1995], however we present the exact definition/algorithm we used for the discrete Allan variance.

Let  $y = (y_i)_{i=1}^N$  be a sequence. For each integer  $\tau$ ,  $1 \leq \tau \leq [N/4]$ , define  $K = [N/\tau]$  (where  $[ \cdot ]$  denotes integral part) and define the sequence of cluster means  $(z_j)_{j=1}^K$  by

$$z_j = \left( \frac{1}{\tau} \right) \sum_{k=(j-1)\tau+1}^{j\tau} y_k.$$

The Allan variance of the sequence  $y$  with time step  $\tau$  is defined by

$$\sigma_y^2(\tau) = \frac{1}{K-1} \sum_{i=1}^{K-1} (z_i - z_{i+1})^2.$$

For the particular Allan variance examples below, the  $y$ 's are the summed raw gyro rates mentioned above.

### LN-200 Analysis

A raw time-series plot for one LN-200 gyro is presented in Figure 1. This particular data sample is taken over 60 hours. The data show no long-term drifts of any kind. Figure 2 shows the Allan variance for all three axes for the LN-200 FOG gyros. All three gyros are nearly identical from an Allan variance standpoint. The Allan variance chart exhibits a slope of  $-1$  and therefore confirms the general impression that the data are mostly uncorrelated noise [IEEE, 1999]. The Allan variance chart ends at 10,000 seconds.

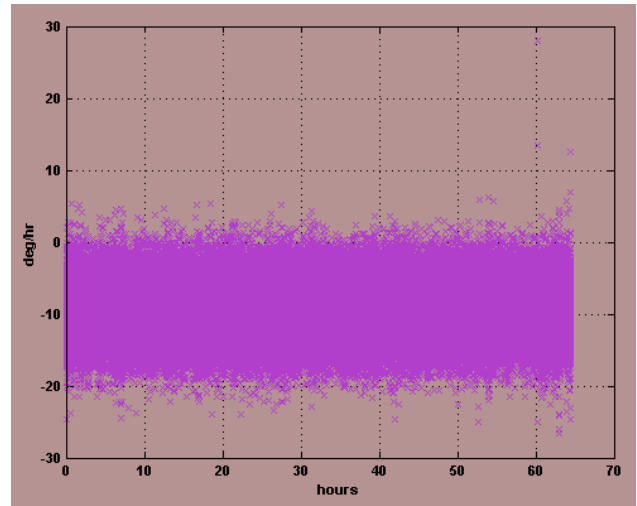


Figure 1: Raw LN-200 data, z gyro.

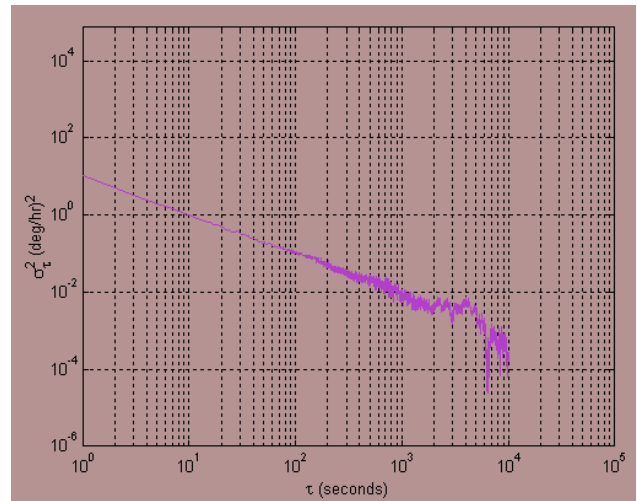


Figure 2: Allan variance, LN-200 z gyro.

The nature of the Allan variance curve suggests that the LN-200 gyro can be modeled as  $K + R(n)$  where  $K$  is a constant and  $R$  is a time term typically referred to as rate noise [IEEE, 1995]. The parameters we determined are  $K = 7 \text{ (deg/hr)}^2$  variance and  $R = 18 \text{ (deg/hr)}^2$  variance. Once that is done, a simulation with the pre-described statistics can be generated. The results of the Allan variance of the simulation are in cyan in Figure 3 and show extremely good agreement.

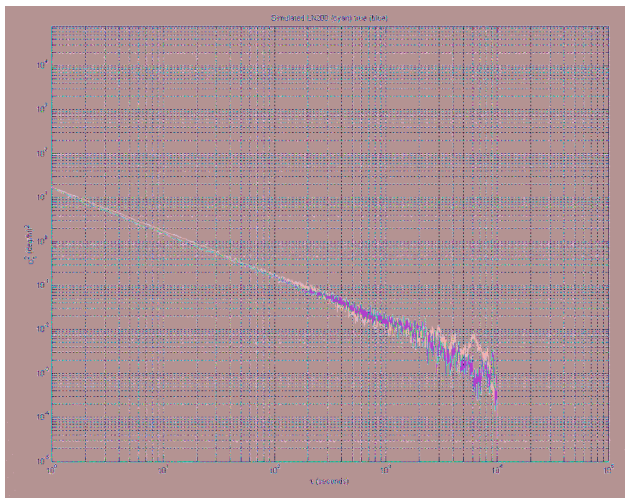


Figure 3: Simulated Allan variance in cyan.

### HG1900 Analysis

The data were collected at the same time and under the same circumstance as the data collection of the LN-200. A raw time-series plot for one Honeywell HG1900 gyro is presented in Figure 4. A more detailed plot showing only the first five hours is presented in Figure 5. There appears to be an initial rate ramp off, however, the same type of behavior occurs at different points in the time series. Therefore, in general, no attempt was made to try to characterize this initial transient.

The Allan variance for the HG1900 gyros is shown in Figure 6. This chart shows all three axes for one of the sample runs. The x axis data are stopped at 10,000 seconds. The first impression of the Allan variance chart is that the curve is nominally flat and hence suggests that the dominant noise source is 1/f noise. However, detailed simulation suggests a more complicated picture as will be described below. However, the more or less constant slope of the HG1900 has important ramifications for the overall system accuracy. The fact that the Allan variance curve stays more or less constant over time suggests that a lower bound of the ability of the end user to estimate the gyro bias is limited at about 1 to 5 degrees per hour. Hence, a navigation system that reaches that accuracy using Kalman filter techniques should be considered “best possible.”

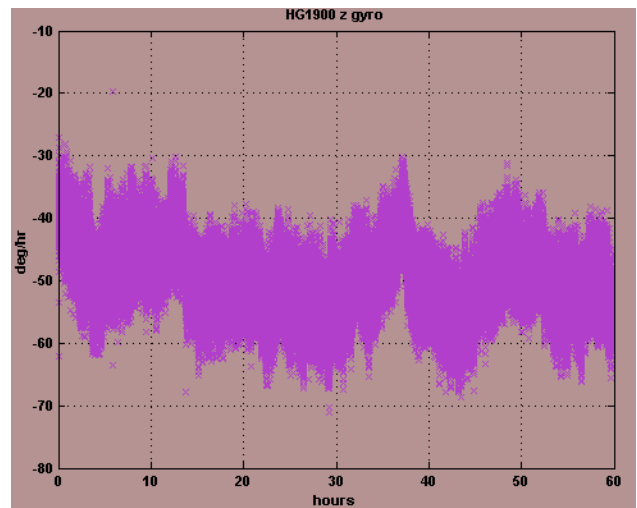


Figure 4: Raw HG1900 data, z gyro.

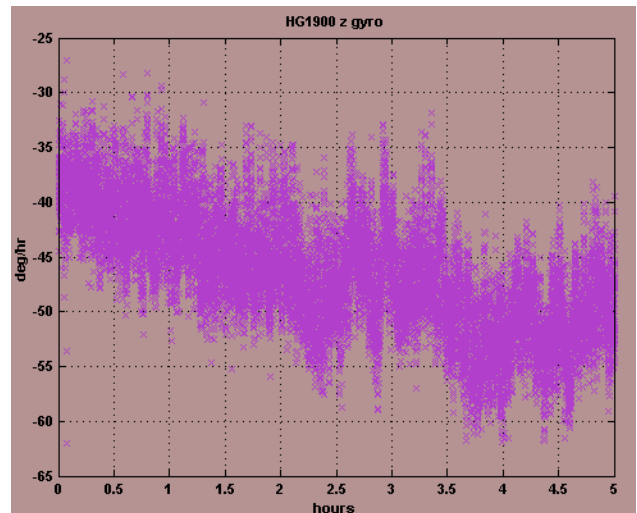


Figure 5: Raw HG1900 data, z gyro, 5 hours.

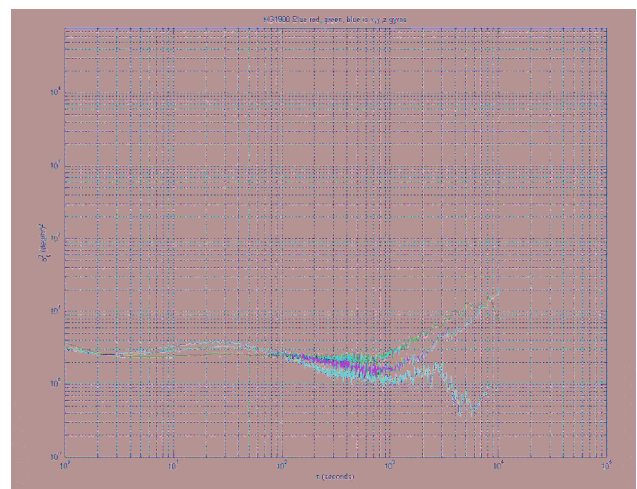


Figure 6: HG1900 Allan variance all axes.

The predominant characteristics of the Allan variance curve are approximately as follows: time 1 to 5 seconds, rate noise; time 5 to 900 seconds, correlated gyro bias; time 900 to 1000 seconds, flicker floor; time 1000 to 10000 seconds, rate random walk. As such, a discrete time model for the gyros can be based on the following five terms

$$r(k) = K + R(k) + C(k) + F(k) + W(k) \text{ where}$$

- $K$  is constant gyro bias
- $R$  is rate noise
- $C$  is correlated noise
- $F$  is bias instability
- $W$  is rate random walk

where the terminology is the same as in IEEE [1995]. The models for each of these terms with time varying characteristics will now be shown.

- $R$  is modeled simply as a Gaussian random sequence,  $R(k) = w(k)$ , where  $w(k)$  is a real Gaussian sequence with  $E(w^2) = \sigma^2$  and  $E(\cdot)$  denotes expectation.
- $C$  is based on the linear Gauss-Markov process  $\dot{x} = -\beta x + \sqrt{2\sigma^2\beta}u$ , where  $u$  is a normal process with  $E(u^2) = \sigma^2$ . The equivalent discrete time realization is given by:
 
$$x(k+1) = Cx(k) + w_k, k = 0, 1, 2, \dots \text{ where } C = e^{-\beta\Delta t},$$
 and  $w_k$  is a normal sequence with variance  $\sigma^2(1 - e^{-2\beta\Delta t})$  [Brown and Hwang, 1992].
- $F$  is a flicker process and to model it we used the technique from Kasdin and Walter [1992]. We deviate slightly from what the IEEE calls bias instability in that we use a cutoff frequency of 0. The flicker process we model is characterized by 1/f power spectral density and 0 slope on the Allan variance chart.
- The rate random walk term is the limiting case in  $C$  as  $\tau \rightarrow \infty$  above and is modeled simply as  $\dot{x} = u$  where  $u$  is a normal process with  $E(u^2) = \sigma^2$ .

Several minimum variance techniques have been developed to find the coefficients of  $R$ ,  $F$  and  $W$  [Vernotte et al., 1992]. These techniques were largely developed for precision oscillators where epoch to epoch correlation is minimal. Due to the presence of the correlated noise term  $C$ , we resorted to an ad hoc approach to determine the coefficients. The values found for these individual terms are as follows:

- $R$  is Gaussian noise with variance .49 (deg/hr)<sup>2</sup>

- $C$  is time constant 19.4 seconds and driving noise with variance 0.00392 (deg/hr)<sup>2</sup>
- $F$  is simulated as 1/f noise with variance 3.61 (deg/hr)<sup>2</sup>.
- $W$  is random walk with driving noise variance 3.82e-4 (deg/hr)<sup>2</sup>.

The results of the simulation are shown in Figure 7. There, the cyan curve is the simulated curve. The agreement is excellent up to 1000 seconds. After 1000 seconds, the curve drops off slightly but this is largely due to this particular instance of the random sequences used to drive the simulation. To further verify the integrity of the simulation, the power spectral density of the curves was considered. To simplify the analysis, we used the MATLAB function *psd* with the default options. The results are shown in Figure 8. The values at low frequency do not agree due to the data biases. For ease of comparison, Figure 9 shows the Allan variance curve of the HG1900 and the LN-200 on the same curve.

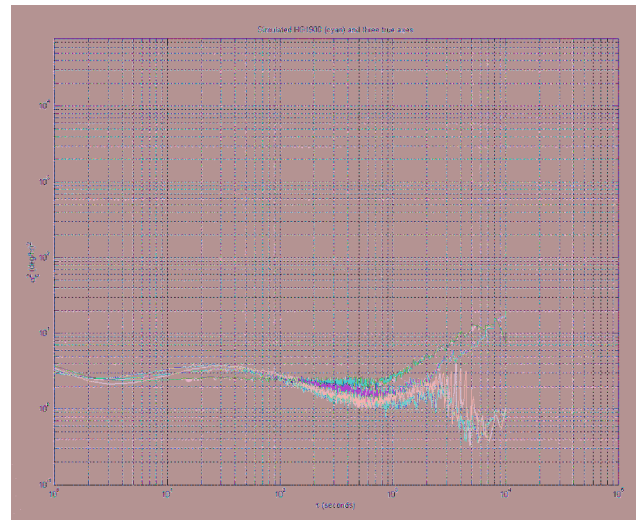


Figure 7: HG1900 simulated Allan variance in cyan.

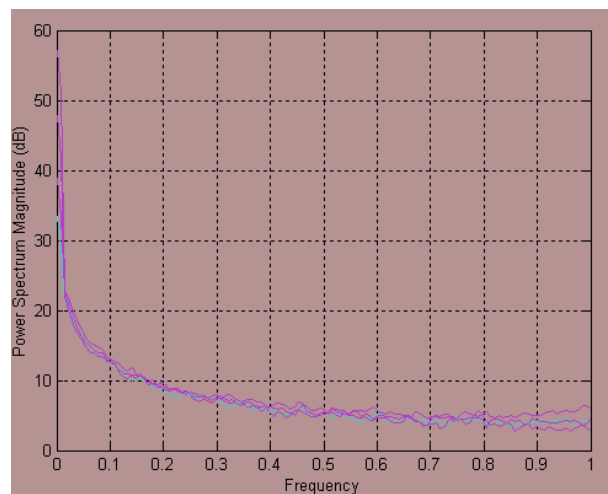


Figure 8: HG1900 gyro and simulation psds.

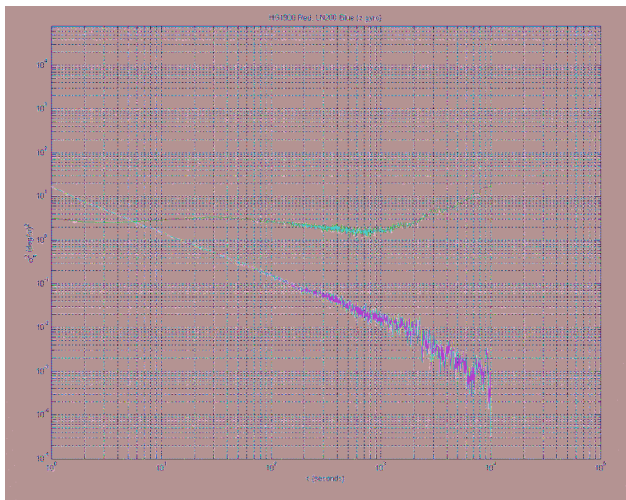


Figure 9: LN-200 and HG1900 Allan variances.

### GPS/INS INTEGRATION

The INS/GPS systems being tested in this paper consist of tactical grade IMUs coupled with an Omnistar aided NovAtel OEMV receiver and a microcomputer to combine the GPS and IMU data. The legacy package is shown in Figure 10. The overall package length was shrunk for the HG1900 (Figure 11). The units weigh about 10 pounds including battery power adequate for four hours of run time. The units can also output real-time data and accept external DC power for longer run times. An additional feature in the systems is the ability to record raw data for post-processing. This feature allows an additional performance criterion to be estimated. A much more compact package is being developed for the smaller HG1930.

The embedded software has a modular design allowing quick prototyping for different inertial sensors. Data rates and various other real-time parameters are set via external controller/viewer software (Figure 12).



Figure 10: LN-200 package.



Figure 11: HG1900 package.

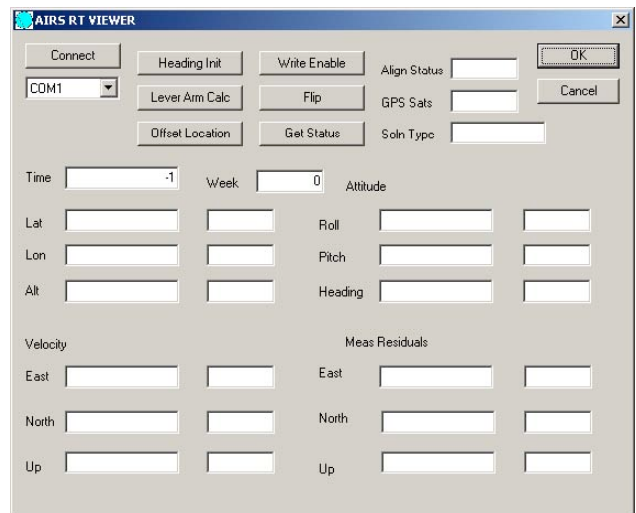


Figure 12: Controller/viewer software.

The results detailed below used GPS outputs from the Omnistar/NovAtel receiver running in the VBS/XP modes. In the VBS mode the receiver's horizontal accuracy was approximately one meter in good environments, and somewhat worse than that in partially obscured environments. In clear conditions with continuous L1 and L2 tracking the receiver will go to XP mode after a number of minutes. After approximately 10 minutes of continuous XP use, this receiver gave horizontal accuracies of about 30 cm. Loss of too many satellites will result in the Omnistar going from XP to VBS mode. The return to XP mode can be as little as two minutes, although in some cases it is appreciably longer. A limited number of experiments were performed using an L1 receiver with no corrections and RTK (Real Time Kinematic) GPS.

The Kalman filter in the real-time software has 15 states, three each for position errors, velocity errors, tilt errors, accelerometer bias, and gyro bias. A more detailed description of the Kalman filter used in integrating the GPS and IMU appears in Strus et al. [2002].

### KALMAN FILTER MODIFICATIONS FOR HG1900

The LN-200 gyros are adequate to perform stationary alignment error estimation by gyrocompassing. This usually results in an initial azimuth error of one to two degrees. The HG1900 does not produce a useful gyrocompassing result due to the large turn-on bias. A motion alignment capability was thus added for the HG1900. Moreover, additional compensation algorithms were added for the potentially large initial uncertainties when motion alignment was not desired.

Based on the Allan variance analysis above, proper gyro modeling requires three states for each Honeywell gyro. Process noise models converting Allan variance parameters to Kalman filter parameters are considered in van Dierendonck et al. [1984]. These models are exact for a single fixed time step of length  $dt$ , but tend to overestimate the covariance data on multiple iterations. Based on these design constraints, we opted for a state reduction model. Reduction models of this type are considered in Greenspan [1996]. Gyros are simply modeled as Gauss/Markov processes with a large time constant. This allows us to tune the filter bias uncertainty to a value very close to that predicted by the Allan variance. In our experience, the decrease in complexity is a reasonable compromise.

### TRUTH SYSTEMS

Two different truth systems for verifying the accuracy of the system were used. For moving and static ground tests the systems were mounted on a 4.6 meter boom on a minivan. The boom has L1/L2 GPS antennas on each end so that the system can be tested against a long baseline GPS attitude system with an estimated accuracy of  $0.06^\circ$  in azimuth, and  $0.12^\circ$  in pitch for a single measurement. The RTK algorithms are described in Sinko [2003] and Basnayake et al. [2006]. The boom can be swung in both azimuth and pitch so that it can be aimed at distant landmarks as shown in Figure 13. The two black boxes on the boom are the IMU/GPS units. For static ground tests the boom has a telescopic rifle scope to sight distant landmarks. With good GPS positional accuracy (within one meter) of the landmark and the vehicle and with the landmark being at least 10 km away, the estimated accuracy of the pointing system is  $0.015^\circ$ .



Figure 13: Boom being sighted.

### TEST RESULTS

Figure 14 shows about 100 minutes of data collected on streets and in a parking lot with good sky coverage. It also illustrates a number of performance characteristics of the two IMU/GPS units under test. The interval from 340500 to 341500 traversed about 10 km of city streets and expressways and some freeway. GPS availability ranged from poor to good and only VBS mode was attained. During this time the Kalman filters in each unit did a reasonable job of estimating the IMU gyro biases. At 341940 the vehicle was stopped and the boom was pointed to a landmark at an azimuth of  $83.75$  degrees. The vehicle remained stationary for about 1000 seconds. During this time the LN-200 based unit drifted very little, while the HG1900 based unit drifted over a degree—as predicted by the Allan variance tests.

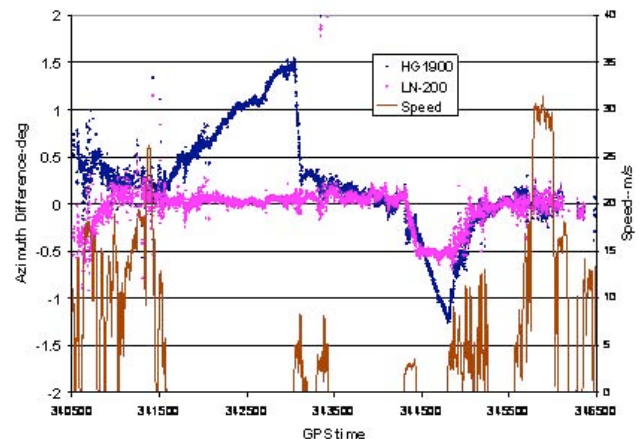
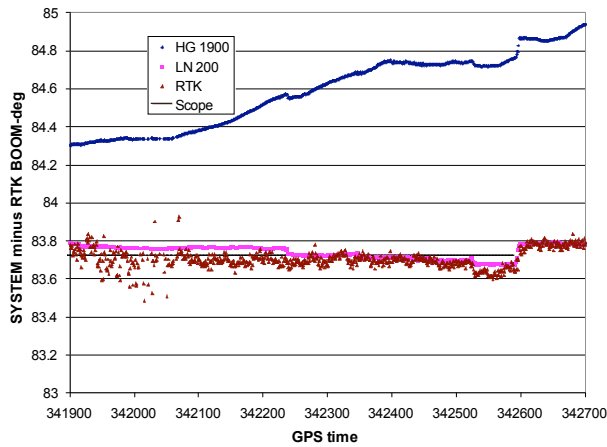


Figure 14: A 100-minute test run.



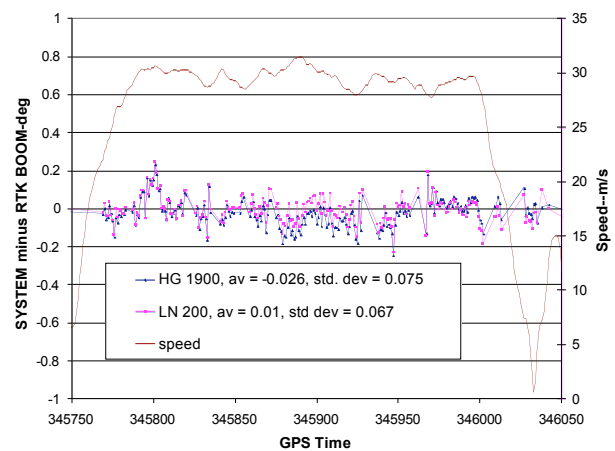
**Figure 15:** Gyro drift while boom was stationary.

Figure 15 shows how the units performed with respect to the telescopic gun sight, at least until 342237 at which time the wind shifted the boom slightly. Another slight wind jump occurred, and then the boom was manually set back to the original azimuth at 342600. After five minutes of driving the IMUs were reasonably well aligned again and little drift was observed over a 1000-second near static period. The van was stationary, but the boom was pointed at several landmarks. The HG1900 started a bit off and drifted through the actual azimuth. Figure 14 details significant gyro runoffs beginning at time 344350. This was caused by making ten successive left-hand circles at the minimum turn radius of the minivan. Our interpretation is that this error is due to scale factor error, since the  $0.25^\circ$  to  $0.5^\circ$  error is in the realm of what would be expected based on the manufacturer’s specifications in Table 1.

After another eight minutes of slow speed driving (less than 10 m/s), a few more static tests were made and then the van was driven on a mostly unobscured freeway for about four minutes. Although the GPS has correlated multipath error when it is stationary, there are indications that this error can be averaged down with dynamics. Extensive testing of a 1.2 meter GPS attitude system indicates that the short term (minutes) bias error is typically  $0.25^\circ$  and the standard deviation is also about  $0.25^\circ$ . When averaged over a sidereal day, the bias dropped to  $0.06^\circ$  because the phase multipath was averaged over a large part of the sky. When the attitude system is moved significantly in azimuth, a similar multipath averaging effect occurs. Translating these results to the 4.66 meter baseline used in these experiments gives an expected dynamic bias of  $0.015^\circ$  with a standard deviation of  $0.06^\circ$ .

The averaging technique basically uses the stability of the IMU to average the GPS. It is, of course, undesirable to use the unit under test to play a part in determining the accuracy of that unit, but it makes sense to do just that

given the difficulty of measuring azimuth on a moving vehicle. Figure 16 shows the difference between the GPS azimuth and the IMU azimuths for about four minutes on a suburban freeway. While the difference jumps around by about  $0.1^\circ$  on an epoch by epoch basis, averaging over any one minute period reduces the difference to about  $0.03^\circ$ . This approach is affirmed by Figure 17, which shows the elevation angles (pitch) measured by the IMUs and the GPS attitude system. In this case the IMUs are known to be quite accurate (throughout entire runs the two units track each other in elevation within  $0.05^\circ$ ), and the elevation angle given is not very dependent on GPS because the IMUs always have the acceleration of gravity. On the other hand, the GPS attitude system will have an elevation error of about twice the azimuth error (or about  $0.12^\circ$ ) because of the unfavorable DOP (dilution of precision) associated with elevation measurements. Again the average works out to a constant offset (while the IMUs were carefully mounted in azimuth, they were not carefully mounted in pitch).



**Figure 16:** Azimuth difference (IMU/GPS–RTK GPS) during a four-minute freeway drive.

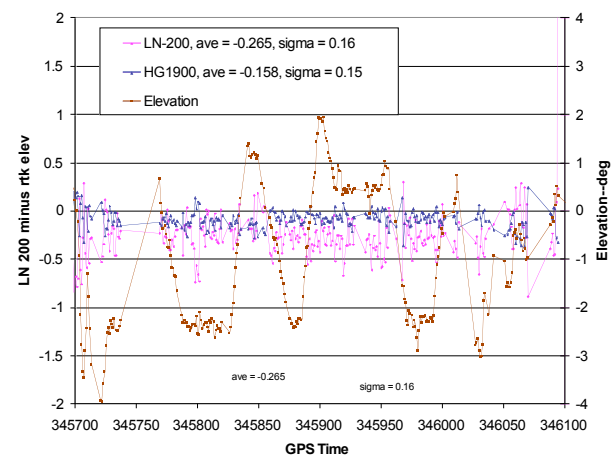


**Figure 17:** Elevation difference (IMU/GPS–RTK GPS) during a four-minute freeway drive.

Rapid turn rates also introduced an error apparently due to residual scale factor error. At low speeds the attitude accuracy was dependent on the accuracy of the GPS measurements, but at aircraft speeds CA code GPS gave attitude accuracies as good as RTK GPS measurements.

## CONCLUSIONS

With suitable dynamics both IMU/GPS systems were capable of providing an azimuth to within at least  $0.06^\circ$   $1\sigma$ . Furthermore, the Allan variance analysis accurately predicted the azimuth drift performance of the IMU systems. While the azimuth is quickly and accurately determined under dynamics, a considerable period of time is required to accurately estimate the gyro bias. This is especially true for the LN-200 because long periods of dynamics can result in a very accurate bias estimate.

The telescopic sight proved a convenient way of testing for static cases. The long boom GPS attitude system, coupled with averaging, appears to give very good testing accuracy during dynamics.

## ACKNOWLEDGMENTS

We wish to thank Patrick Weldon of Honeywell for lending us on short notice the HG1900 unit used in our tests.

## REFERENCES

- Basnayake, C., C.C. Kellum, J. Sinko, J. Strus (2006) GPS-based relative positioning test platform for automotive active safety systems, ION GNSS 2006, pp. 1457–1467.
- Brown, R.G., P.Y.C. Hwang (1992) Introduction to Random Signals and Applied Kalman Filtering, John Wiley & Sons, New York, NY.
- Greenspan, R.L. (1996) GPS and Inertial Integration, in Global Positioning System: Theory and Applications Vol. II, pp. 187–220, (Edited by B.W. Parkinson and J.J. Spilker), American Inst. of Aeronautics and Astronautics, Washington, D.C.
- Honeywell (2004) User's Manual for HG1900BA99, Minneapolis, Minnesota.
- Hou, H. (2004) Modeling inertial sensors errors using Allan variance, Masters Thesis, Univ. of Calgary, Geomatics Engineering, UCGE Report 20201 (available online).
- IEEE Std 647–1995 Annex C: IEEE Standard Specification Format Guide and Test Procedure for Single-Axis Laser Gyros—An Overview of the Allan Variance Method of IFOG Noise Analysis.
- IEEE Std 1139–1999 IEEE Standard Definitions of Physical Quantities for Fundamental Frequency and Time Metrology—Random Instabilities.
- Kasdin, N.J., T. Walter (1992) Discrete simulation of power law noise, 1992 IEEE Frequency Control Symposium, pp. 274–283.
- Litton (2000) LN-200 Inertial Navigation Measurement Unit, Source Control Document, Woodland Hills, California.
- Sinko, J.W. (2003) RTK performance in highway and racetrack experiments, Navigation, Vol. 50, No. 4, pp 265–275.
- Strus, J.M., E.G. Blackwell, C.A. Gellrich, M.R. Kirkpatrick, J.W. Sinko (2002) Instrumentation of paratroopers and large pallet loads, ION GPS 2002, pp 2457–2465.
- van Dierendonck, A.J., J.B. McGraw, and R.G. Brown (1984), Relationship between Allan variances and Kalman filter parameters, Proceedings of the 16<sup>th</sup> Annual Precise Time and Time Interval (PTTI) Applications and Planning Meeting, NASA Goddard Space Flight Center, pp 273–293, Accession Number 85N29238.
- Vernotte, F., E. Lantz, J. Gros Lambert, J.J. Gagnepain (1992) A new multi-variance method for the oscillator noise analysis, 1992 IEEE Frequency Control Symposium, pp 284–288.